Dynamic regulation of ERK2 nuclear translocation and mobility in living cells

Mario Costa[1], Matilde Marchi[2,3], Francesco Cardarelli[2,3], Anusrhee Roy[4], Fabio Beltram[2], Lamberto Maffei[1,5] and Gian Michele Ratto[1,*]

[1]Institute of Neuroscience CNR, Via Moruzzi 1, 56100 Pisa, Italy
[2]NEST, Scuola Normale Superiore, Pisa, Italy
[3]Italian Institute of Technology, Italy
[4]Department of Physics and Meteorology, Indian Institute of Technology, Kharagpur, India
[5]Laboratory of Neurobiology, Scuola Normale Superiore, Pisa, Italy
*Author for correspondence (e-mail: gimmi@in.cnr.it)

Accepted 20 September 2006
Journal of Cell Science 119, 4952-4963 Published by The Company of Biologists 2006
doi:10.1242/jcs.03272

Summary

The extracellular signal-regulated protein kinase ERK1/2 is a crucial effector linking extracellular stimuli to cellular responses: upon phosphorylation ERK [also known as mitogen-activated protein kinase P42/P44 (MAPK)] concentrates in the nucleus where it activates specific programs of gene expression. Notwithstanding the importance of this process, little is known about the modalities, time course and regulation of ERK exchange between nucleus and cytoplasm in living cells. We visualized the dynamic of nuclear translocation by expressing low levels (<150 nM) of fluorescently tagged ERK2 in living fibroblasts. Time-lapse imaging demonstrated that nuclear concentration can change bidirectionally with a time constant of a few minutes. The increase of nuclear concentration requires continuous MEK (also known as MAPK kinase) activity upstream of ERK and is rapidly reduced by the operation of phosphatases. We measured quantitatively the speed of ERK2 shuttling between nucleus and cytoplasm and determined that shuttling accelerated after ERK activation, becoming fast enough not to be rate-limiting for translocation. Finally, we demonstrated that ERK2 did not diffuse freely in the nucleus and that diffusion was further impeded after phosphorylation, suggesting the formation of complexes of low mobility. These results show that nucleo-cytoplasmic trafficking of ERK2 and its mobility are dynamically regulated in living cells.

Supplementary material available online at
http://jcs.biologists.org/cgi/content/full/119/23/4952/DC1

Key words: Phosphorylation, Signal transduction, Nuclear transport, Kinase, Phosphatase, MAP kinase

Introduction

The extracellular signal-regulated protein kinase ERK1/2 [P42/P44 mitogen-activated protein kinase (MAPK)] is one of the main transducers of extracellular signals linking the stimulation of membrane-bound receptors to changes of cellular function (Robinson and Cobb, 1997; Roux and Blenis, 2004). The ERK1/2 pathway integrates various cytosolic signals: depending on the cellular context, the PKC and PKA pathways and intracellular calcium contribute to ERK1/2 modulation, thus realizing a complex signalling network (Bhalla and Iyengar, 1999; Chuderland and Seger, 2005). This plethora of incoming signals is converted to a variety of actions, owing to the phosphorylation of downstream effectors both in the cytoplasm and in the nucleus: indeed, the ubiquitous nature of ERK1/2 action is underlined by the ever-expanding list of ERK1/2 substrates. The long-term actions of ERK1/2 are accomplished by promoting the expression of genes under specific transcription factors, including Elk-1, Myc, Myb and the cAMP-response element (CRE). Activation of gene expression is preceded by the translocation of activated ERK1/2 in the nucleus (Chen et al., 1992; Lenormand et al., 1993); this step is necessary for the correct control of gene expression by growth-factors (Brunet et al., 1999; Kim et al., 2000), for morphological transformation of fibroblasts (Cowley et al., 1994) and for neurite extension in PC12 (Robinson et al., 1998). Furthermore, disruption of ERK2 localization in the nucleus severely affects the transduction of ERK2 signalling (Fukuda et al., 1997a).

Since ERK is activated in the cytoplasm in response to stimuli transduced at the level of the cell membrane, the trafficking between cytoplasm and nucleus determine the efficiency of the transfer of ERK activation state to the nuclear compartment. Surprisingly, notwithstanding the centrality of the process of ERK1/2 translocation, most of the dynamical details of this event are still unknown. Indeed, the first direct observation of ERK1/2 permeation through the nuclear membrane of living cells has been attained only very recently (Ando et al., 2004), and although it has been proposed that ERK1/2 continuously shuttles between the cytosolic and nuclear compartment (Volmat et al., 2001), the kinetic, regulation and functional consequences of this process are still to be fully comprehended.

To study the mechanisms underlying the spatiotemporal dynamic of ERK2 localization and regulation we have tagged ERK2 with green fluorescent protein (GFP) to image localization and mobility of ERK2-GFP in living cells. In this

study we have minimally perturbed the cells by employing very low-level expression of ERK2 (≤150 nM) to avoid altering the relative abundance of ERK2 compared with the upstream and downstream elements. We found that upon stimulation, ERK2-GFP localized in the nucleus with a dynamic that depended on the temporal and biochemical characteristics of the stimulus. This process required continuous activation of the MEK (also known as MAPK kinase)/ERK1/2 pathway, since blockade of MEK activity with a specific inhibitor rapidly reverted nuclear localization indicating the presence of a fast turnover of ERK2 phosphorylation. Photobleaching of the nucleus was followed by rapid recovery of the fluorescence, and the speed of this process was increased by a factor of two after stimulation. These data, in agreement with recent experiments (Ando et al., 2004), conclusively demonstrate that ERK2 shuttles between the cytosol and the nucleus in an activity-dependent manner. Finally, we found that minutes after stimulation the apparent diffusion coefficient of ERK2 in the nucleus diminished, indicating its binding to molecules of limited mobility. Our experiments demonstrate that ERK phosphorylation and nuclear concentration reflect the state of activation of the signalling network with great temporal fidelity. This is accomplished by the rapid regulation of protein flux across the nuclear membrane and the binding to low-mobility substrates.

Results

Nuclear accumulation of ERK-GFP following stimulation

We fused ERK2 (p42 MAPK) with a fluorescent tag and this construct was transfected in NIH-3T3 cells. Initially we observed that ERK2-GFP in non-stimulated cultures always concentrated in the nucleus of brightly fluorescent cells (Fig. 1A). This effect was saturable [we never observed a concentration index (CI)>2.2, even in extremely bright cells], and it is because of the disruption of the relative ratios of MEK and ERK concentration (Fukuda et al., 1997b; Lenormand et al., 1993; Rubinfeld et al., 1999). In previous studies this problem was either ignored (Ando et al., 2004) or overcome by co-expressing MEK1 to rescue this unbalancing (Burack and Shaw, 2005; Horgan and Stork, 2003), thus introducing another exogenous protein. Instead, we identified the upper limit of ERK2-GFP expression that was compatible with a normal pattern of ERK2 localization in starved cells (Fig. 1B). The concentration of ERK2-GFP was estimated by comparing the fluorescence of the cells with artificial cells loaded with known concentrations of enhanced green fluorescent protein (EGFP) (supplementary material Fig. S1). These data demonstrate that ERK2-GFP localisation was normal up to approximately 150 nM, and that nuclear accumulation saturated at a concentration larger than 1.5 μM. In approximately 80% of the cells included in the study the concentration of ERK2-GFP was ≤100 nM. Since ERK levels in mammalian cells have been estimated to be in the 1-3 μM range (Ferrell, Jr, 1996; Whitehurst et al., 2002), ERK2-GFP was much less abundant than the endogenous protein. The dotted line in Fig. 1 represents the upper level of expression that we accepted in our experiments (150 nM); these cells were very weakly fluorescent and required great care to attain good imaging. In addition, we have excluded cells that, notwithstanding the low fluorescence, exhibited visible nuclear accumulation in the starved state. As expected, the phosphorylation and localization of ERG2-GFP, in weakly fluorescent cells, depended on the activation of the ERK pathway (supplementary material Fig. S2) and the subcellular localization of ERK-GFP was identical in the N- and C-terminus fusion proteins (supplementary material Fig. S2G).

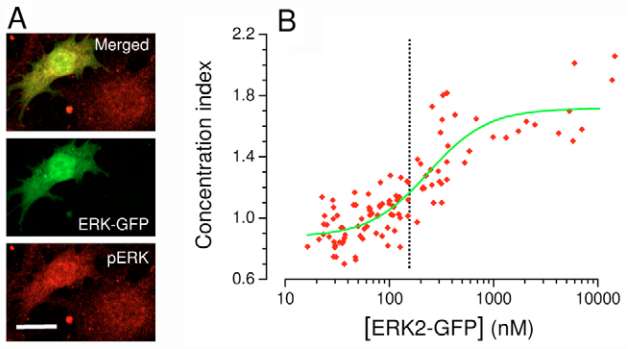

Fig. 1. Estimate of ERK2-GFP concentration. (A) Starved cells with an high expression of ERK2-GFP exhibited strong nuclear localization (green), independently of ERK phosphorylation (red, pERK immunofluorescence). Bar, 20 μm. (B) Relationship between the concentration of ERK2-GFP and nuclear localization in starved cells. The concentration index (CI, see Materials and Methods) measures ERK2-GFP localization: a larger CI corresponds to stronger nuclear accumulation. To extend the measures over two orders of magnitude we used variable laser power according to the best imaging conditions for each cell; data were pooled together after normalization to reference imaging conditions. The concentration of ERK2-GFP was estimated by comparing the fluorescence of the cells with artificial cells loaded with known concentrations of EGFP (supplementary material Fig. S1). In this study we selected cells with expression level less than approximately 150 nM (broken line) and that had a CI≤1 when starved.

The dynamics of nuclear accumulation were studied in time-lapse experiments. Stimulation was provided by adding either serum or fibroblast growth factor 4 (FGF4) (80 ng/ml in all experiments) to the medium. After an initial latency ($T_{10\%}$ ranging between 2 and 4 minutes) ERK2-GFP rapidly concentrated into the nucleus, reaching 90% of response within 9 minutes of the onset of stimulation (Fig. 2A,B; supplementary material Movie 1) following an exponential time course (see later). Cumulative data of the response onset are shown in Fig. 2B. The translocation of the N- and C-terminal fusion proteins followed a similar time course (compare the green traces in Fig. 2B). This experiment was also performed with analogous results (Fig. 2B, red line) in a cell line (ERK1-KD) stably transfected with a short hairpin RNA (shRNA) directed at interfering with ERK1 expression (Vantaggiato et al., 2006). Furthermore, to confirm the generality of the result, similar time courses have been observed in two additional cell types: NIH-L1 preadipocytes and primary fibroblasts (supplementary material Fig. S3).

We compared the responses induced by serum and FGF in 3T3 cells: initially, serum and FGF4 produced similar responses activating a monotonically increasing translocation. At a later time the serum-induced response declined gradually, whereas FGF4 caused constant accumulation during the imaging period (up to 2 hours, Fig. 2C-E).

We tested the temporal fidelity of nuclear accumulation to the stimulus temporal profile by treating the cells with a brief presentation of FGF4. Cells were continuously perfused and

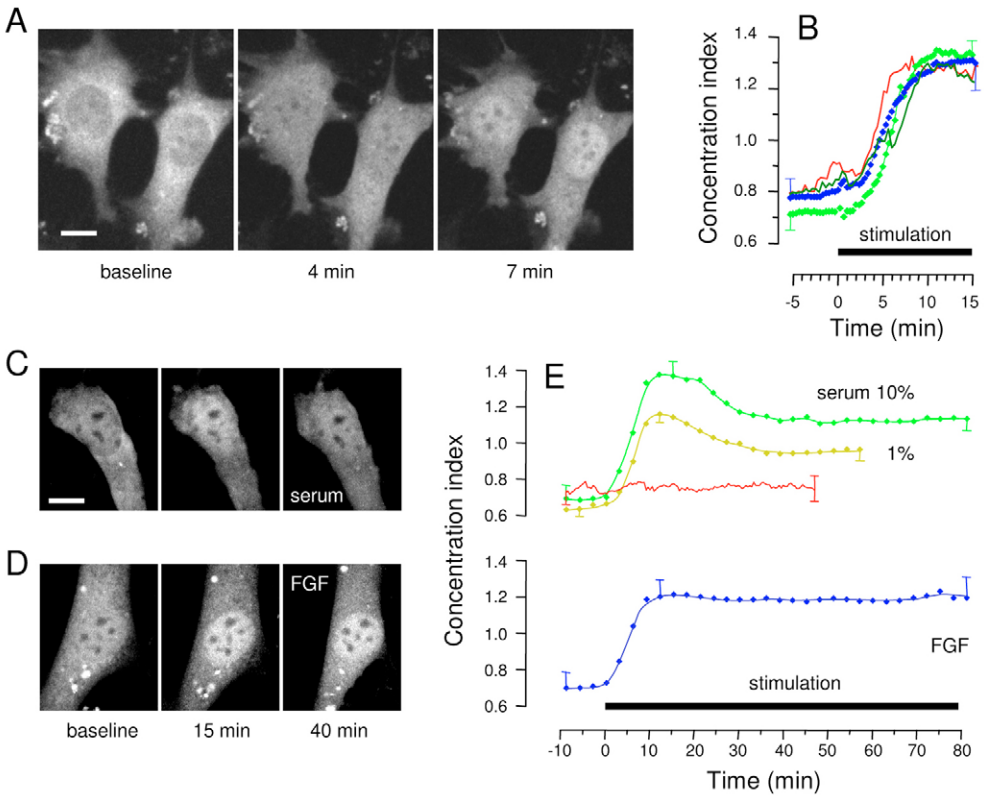

Fig. 2. ERK2-GFP concentrates in the nucleus of living cells after stimulation. (A) Nuclear fluorescence increased within 4 minutes from stimulation with 10% serum. Bar, 10 μm in all panels. (B) Cumulative time course of the CI after stimulation with FGF4 (blue, *n*=9; ERK1-KD, red line, *n*=4) or 10% serum (green symbols, *n*=15; C-ERK2, dark-green line, *n*=6). In this and following figures, the vertical bars are representative of the s.e.m. at various time points. (C,D) The CI after stimulation with serum had a transient component (30% decline 40 minutes after stimulation), whereas FGF4 produced a sustained response. (E) Time course of ERK2-GFP nuclear concentration after stimulation with two different doses of serum (green, 10%, *n*=7; yellow, 1%, *n*=8) and FGF (blue, *n*=8). Red trace, untreated control cells (*n*=9).

stimulated with FGF for only 4 minutes (Fig. 3). Initially, ERK-GFP concentration in the nucleus increased like the response to a stationary stimulus. However, soon after peak the CI declined exponentially almost to baseline level following the temporal modulation of the activating stimuli.

ERK localization is dynamically controlled by the activation of the upstream pathway

The translocation of ERK2-GFP required activation of the upstream kinase MEK1 since the selective inhibitor of MEK, U0126 (English and Cobb, 2002), blocked nuclear accumulation (supplementary material Fig. S4A,B). In starved cells the upstream pathway is not necessarily totally deactivated: ERK might be regulated by the dynamic equilibrium of a moderate basal activity of the Receptor-Ras-MEK1-ERK1/2 module with competing phosphatates. This putative basal activity should be revealed by the blockage of dephosphorylation. Indeed, upon perfusion of starved cells with 1 mM of the phosphatase inhibitor sodium-orthovanadate (Schramek et al., 1996), ERK2-GFP began to accumulate in the nucleus within a few minutes (Fig. 4A). This process occurred in parallel with ERK activation, as demonstrated by immunohistochemistry with the pERK antibody (supplementary material Fig. S4C,D). The accumulation of ERK2-GFP in the nucleus gradually increased throughout the duration of the imaging period (up to 1 hour). This demonstrates that even after 24 hours of serum deprivation, the ERK1/2 pathway is undergoing some basal activation that is equilibrated by a corresponding level of phosphatase activity. The change in CI is remarkably well described by an exponential growth (τ=26 minutes; Fig. 4C). During pretreatment with U0126 we did not detect any decrease in the CI (supplementary material Fig. S4B). This might be because of a very low regulation of phosphatases in starved cells or the presence of a fraction of ERK immobilized in the nucleus (see later).

If a similar dynamical equilibrium between phosphorylation and dephosphorylation holds also after activation, it would be expected that the sustained nuclear accumulation caused by FGF4 would require continuous activation of the MEK1-ERK1/2 pathway. We treated the cells with U0126 after 15 minutes of stimulation with FGF4 (Fig. 4B, supplementary material Movie 2), which caused an immediate decrease in ERK-GFP concentration in the nucleus. The speed of this process showed that U0126 diffused rapidly in the intracellular medium and that its effect was very fast. More importantly, this experiment demonstrated that ERK activation and localization are caused by the balance of two competitive processes of phosphorylation and dephosphorylation and that both processes are rapid. Indeed, the rate of loss of nuclear fluorescence was very high, comparable to the rate observed after FGF-induced response. To allow a better comparison of the time course of these processes, the change in CI in response to these treatments has been normalized between 0 and 1 and has been displayed in Fig. 4C. Time 0 corresponds to the beginning of treatment of naïve cells with FGF4 or orthovanadate and of FGF-treated cells with U0126+FGF. The continuous lines are exponential fits to the experimental data: the time constant of the loss of ERK concentration from the nucleus is 3.0±0.13 minutes (R^2=0.99, blue curve), similar to the FGF-induced response (τ=3.3±0.12 minutes, R^2=0.99, green curve). In comparison, the rate of nuclear accumulation induced by the block of phosphatases in starved cells is much lower (τ=26±0.48 minutes, R^2=0.98, red curve), suggesting

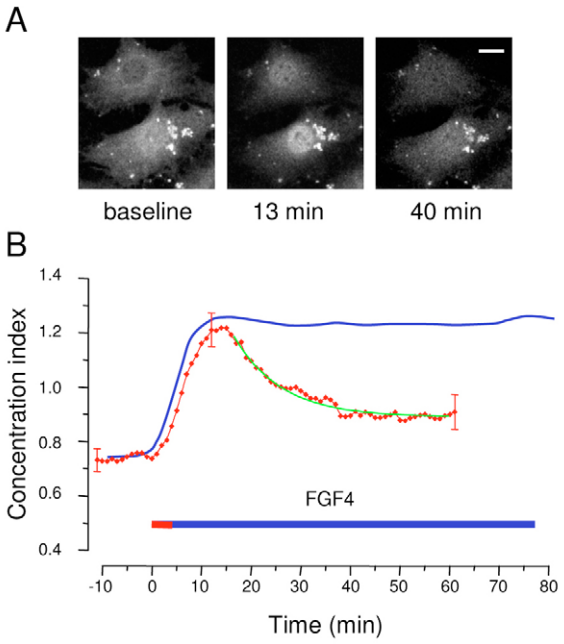

Fig. 3. ERK2-GFP translocation in response to a transient stimulus. (A) Cells have been stimulated with FGF4 for only 4 minutes. Bar, 10 μm. (B) Comparison of the response to 4 minutes (red trace, n=15) or continuous stimulation (blue trace). The green line is an exponential best fit (τ=9.5 minutes, R^2=0.99).

that upon stimulation the rate of ERK2 phosphorylation increased by almost a factor of ten. The latency of the effect of U0126 is virtually zero, demonstrating that imported ERK2 is rapidly dephosphorylated and exported from the nucleus. In normal conditions the response to FGF4 is seen as a sustained translocation because this process is compensated by an equilibrating influx of phosphorylated ERK2; the block of MEK1 unveil these compensating processes. This interpretation has two implications: first, the drop in ERK-GFP concentration caused by U0126 should be inhibited by orthovanadate; and second, nuclear ERK is only partially phosphorylated during steady stimulation with FGF.

These points were explored in the next set of experiments. We stimulated ERK by adding orthovanadate (Fig. 5A). When the cells showed a pronounced increase in nuclear fluorescence we added U0126. In stark contrast to the previous experiment, U0126 stopped but did not revert the increase in nuclear fluorescence. This experiment confirms that phosphatase activity quickly downregulates the active ERK pathway. The continuous operation of phosphatases implies that, after stimulation, the nuclear ERK is only partially phosphorylated; indeed, when cells treated with FGF4 were also exposed to orthovanadate, ERK-GFP concentration in the nucleus further increased by approximately 30% (Fig. 5B). To test for the presence of a fraction of non-phosphorylated ERK2 during maximal stimulation, we separated the phosphorylated and non-phosphorylated pools of ERK by immunoprecipitation (supplementary material Fig. S5). This experiment revealed that 15 minutes after the onset of the stimulus (at the peak of nuclear accumulation) approximately 10% of ERK2 was not phosphorylated. Finally, we investigated the spatial distribution of non-phosphorylated ERK2 by comparing the CI observed by imaging ERK-GFP (total protein) with the CI imaged with the phospho-specific antibody (phosphorylated protein) in cells treated with FGF (Fig. 5C,D). The average translocation measured with the phospho-specific signal is similar in cells expressing ERK2-GFP and in non-transfected cells (CI=1.61±0.07 and 1.72±0.07, respectively; $P \leqslant 0.26$), indicating that the presence of the transgene did not affect ERK1/2 phosphorylation and translocation. We then compared the CI measured in the green and red channels. If the entire pool of ERK2-GFP was phosphorylated we should observe a similar CI in the red and green channels and the observations would cluster around the line of slope 1 (Fig. 5C,D). Instead, all points fall under this line as they are fitted by a slope of 0.49±0.07. The average CI measured in the green channel is 1.46 times larger than in the red (2.35±0.08 versus 1.61±0.07, $P \leqslant 0.0001$ using paired t-test), indicating that 15 minutes after stimulation nuclear ERK2-GFP was not totally phosphorylated. Since the phospho-specific antibody recognizes both ERK1 and ERK2, we repeated the experiment in ERK1-KD cells (blue symbols). Also in the absence of endogenous ERK1 the data points clustered under the line of slope 1, confirming that ERK2 phosphorylation in the nucleus is only partial.

ERK2-GFP continuously shuttles across the nuclear membrane

Recent experiments have shown that ERK shuttles between the nucleus and cytoplasm in an activity-dependent manner (Ando et al., 2004). The shuttling must be fast enough to replenish a pool of nuclear pERK that is dephosphorylated and exchanged with the cytosol through a process with $\tau \approx 3$ minutes. Since the published measures leave substantial uncertainty regarding the velocity of turnover and the presence of an immobile fraction, we addressed these issues by studying the recovery of ERK2-GFP fluorescence after photobleaching of the nucleus. Given that photobleaching is irreversible, any recovery of fluorescence in the nucleus must be because of the influx of unbleached ERK2-GFP from the cytoplasm. Since the protein concentration in the nucleus is left unaffected by photobleaching, this influx is in equilibrium with an equal efflux of bleached chimera and the time constant of the recovery is inversely proportional to the permeability through the nuclear membrane. Fig. 6A shows that ERK2-GFP is continuously exchanged between the nucleus and cytoplasm and that the turnover accelerated after activation, as demonstrated by the time course of the fluorescence recovery before and after stimulation (Fig. 6B). The recovery in all the measured cells was fitted with remarkable accuracy by a single exponential and therefore the recovery process can be described by its time constant τ and asymptotic value. The τ is related to the speed of protein shuttling across the membrane, and it was found to accelerate by almost a factor of two 15-45 minutes after stimulation (Fig. 6C), during a time interval in which the CI remains constant. Cells transfected with the C-ERK construct and ERK1-KD cells showed a similar level of acceleration (Fig. 6C, empty symbol). A similar acceleration of turnover was found in two additional cell types (supplementary material Fig. S6A). Three hours after continuous stimulation with FGF4, τ returned to an intermediate value. The asymptotic value of the recovery

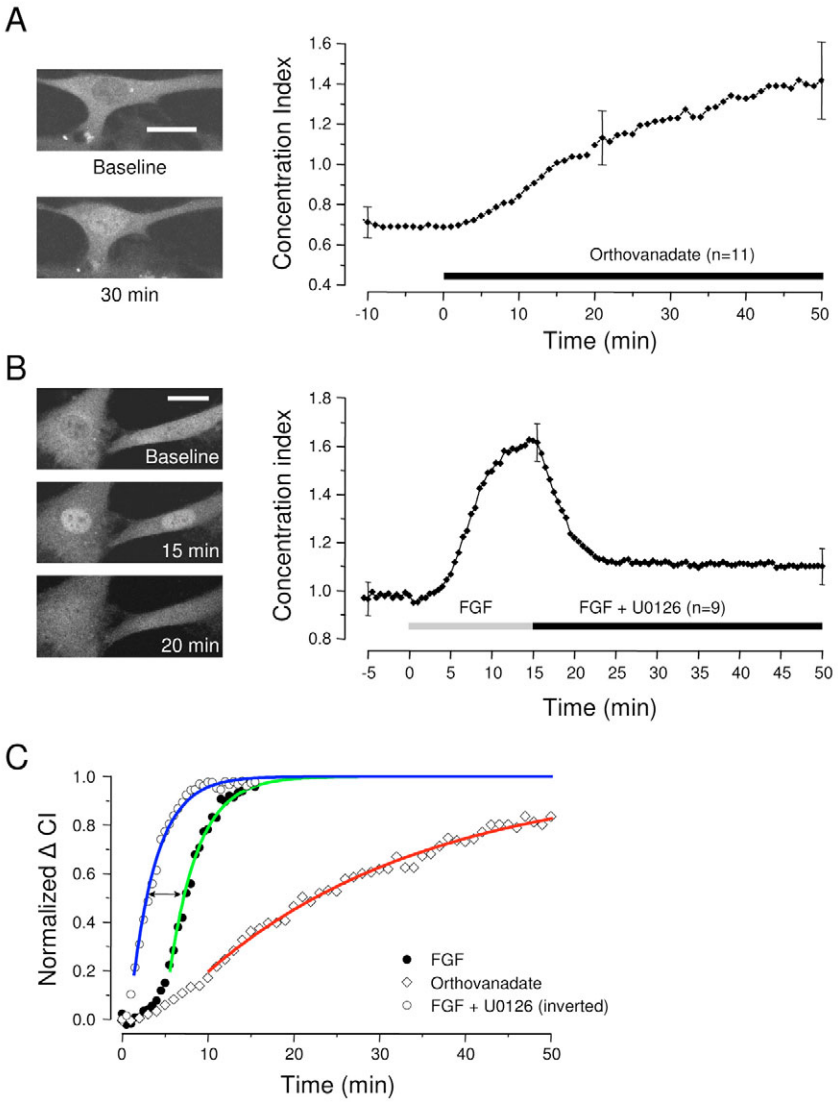

Fig. 4. Dynamic regulation of ERK2-GFP localization. (A) Treatment of starved cells with the phosphatase-inhibitor sodium-orthovanadate caused gradual nuclear translocation. Bar, 20 μm in all panels. (B) ERK activation and consequent nuclear accumulation required continuous activation of the MEK-ERK pathway. Cells were treated initially with FGF4 and with U0126 15 minutes later (20 μM). Blockage of MEK caused the rapid loss of nuclear fluorescence. (C) Comparison of the time course of ERK2-GFP translocation in response to FGF, FGF4+U0126 and orthovanadate. Traces from A and B have been normalized from 0 to 1, with 0 indicating the CI at the time of administration of the specific compound and 1 indicating the asymptotic value of the exponential fits. The CI decline caused by U0126 (open circles) has been inverted for a better comparison with the other data. The continuous lines are exponential fits to the top 80% of the data points.

would be equal to 1 if the pool of nuclear protein was completely exchangeable with the cytoplasm, and it would be <1 in the presence of a fraction of protein immobilized in the nucleus (immobile fraction, IF). Starved cells showed a small but significant IF ($P \leqslant 0.0001$) (Fig. 6D). After stimulation, the IF increased to 12%.

Since the time course of the fluorescence recovery was rather variable, we thought it necessary to perform the fluorescence recovery after photobleaching (FRAP) experiments in the same cell before and after stimulation. The results from the population of cells recorded in paired conditions is reported in Fig. 6E. Each cell is plotted according to its CI and τ of fluorescence recovery in starved condition and after stimulation with serum or FGF4. The time constant of turnover was independent of the concentration of ERK2-GFP in the range we considered in our experiments (ERK2-GFP$\leqslant$150 nM; supplementary material Fig. S6B,C). However, the situation changed in cells strongly overexpressing ERK2-GFP. We found that the IF was zero (IF=0.01, $P \leqslant 0.001$), indicating that ERK2-GFP accumulation was not because of immobilization in the nucleus, and the turnover was significantly slower (Fig. 6C), indicating saturation of the machinery presiding at nuclear import and export. These data stress the importance of operating on cells with minimal expression of ERK2-GFP.

ERK-GFP mobility in the nucleus depends on its activation state

Inactive wild-type ERK is bound to MEK1, which is actively exported from the nucleus by the exportin CRM1 (Adachi et al., 1999; Adachi et al., 2000). This mechanism also operates on the ERK2-GFP chimera as demonstrated by the onset of a gradual accumulation of ERK2-GFP in the nucleus during treatment with the inhibitor leptomycin B (Kudo et al., 1999) (supplementary material Fig. S7A,B). Thus, the cytosolic localization of ERK in starved cells is because of the efflux mediated by CRM1. Although it is well established that CRM1 is required for the depletion of ERK from the nucleus in starved cells, nothing is known about its role in controlling ERK efflux after stimulation. We tested this by pretreating cells with leptomycin, followed by treatment with FGF and U0126 (supplementary material Fig. S7C). If CRM1-mediated export

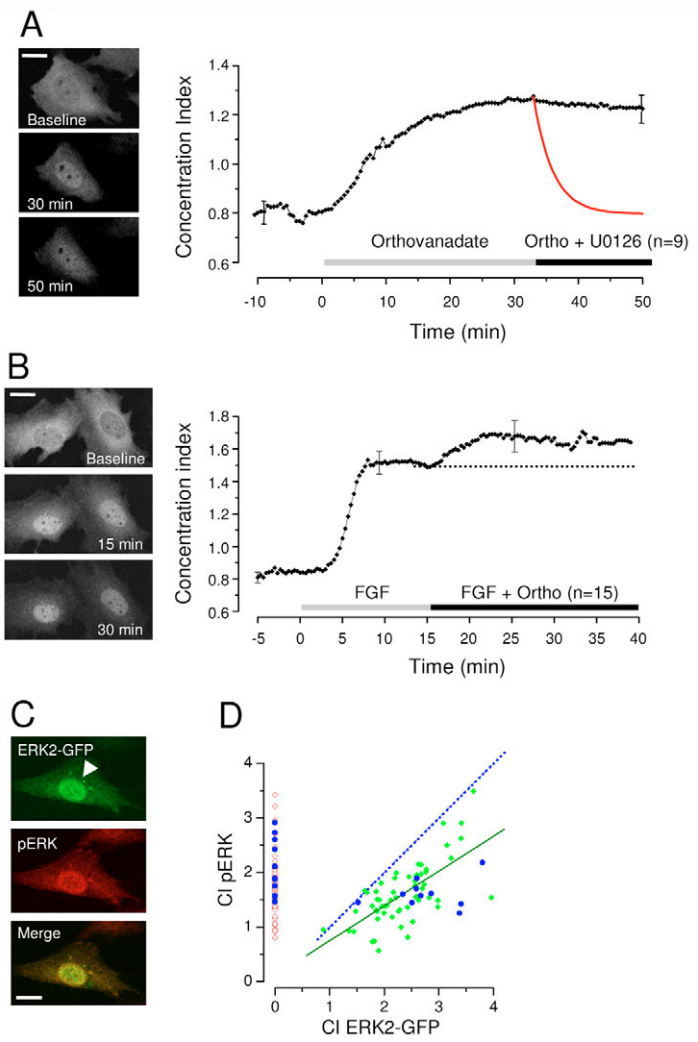

Fig. 5. (A) The MEK inhibitor U0126 did not decrease nuclear ERK2-GFP after orthovanate-induced translocation. Starved cells were treated first with the phosphatase inhibitor and then with U0126 (20 μM). Bar, 10 μm in all panels. The red line represents the decline observed in U0126 in the absence of the phosphatase inhibitor (Fig. 4B). (B) FGF4 alone was not sufficient to cause maximal translocation. Cells were treated initially with FGF4 and with orthovanadate 15 minutes later, which caused a 30% increase in the CI. (C) Relationship between phosphospecific signal and ERK2-GFP localization. Transfected fibroblasts were stimulated with FGF for 15 minutes, fixed and treated for pERK immunofluorescence. (D) CI measured on a sample of 58 transfected and 57 non-transfected cells (green and red dots, respectively). A similar distribution was found in ERK1-KD cells (blue dots).

was the main vehicle of ERK export in activated cells we should observe an inhibition of the response to U126. By contrast, we observed that treatment with U0126 caused an immediate reduction in the nuclear concentration of ERK2-GFP. Although this process might be slightly slower than observed in control conditions (τ=4.47 minutes versus 3.0 minutes in control as from Fig. 5C), these data suggest that a large fraction of ERK2 exit occurs because of bidirectional facilitated diffusion across the nucleoporins independently of CRM1.

The special role of CRM1-mediated export is that it can operate against a concentration gradient. When ERK2 is strongly overexpressed there is a sizable fraction of ERK2 not bound to MEK1 and that is therefore unable to be exported by CRM1. As we have seen, in these conditions ERK2 accumulates in the nucleus and this requires that either its influx occurs against a gradient or that its mobility once in the nucleus is reduced. Furthermore, if the ERK2 effective diffusion coefficient (D_{eff}) was to depend on its phosphorylation state, this would influence the activity-dependent translocation process. We have studied ERK2-GFP mobility by bleaching a small spot of the nucleus with a brief laser pulse (250 milliseconds) and imaging the recovery process in starved cells and after stimulation with FGF4 (Fig. 7). This technique is a very effective tool for measuring the diffusion of nuclear protein and it does not inflict any damage on the analysed cells (Houtsmuller et al., 1999; Koster et al., 2005; Phair and Misteli, 2000). The rate of fluorescence recovery is correlated with the mobility of the fluorescent reporter, with a faster time course being associated with a larger diffusion coefficient (Carrero et al., 2003; Lippincott-Schwartz et al., 2001). The qualitative inspection of the fluorescence recovery indicates that ERK is substantially less mobile than GFP (Fig. 7D,E). Indeed, the recovery of GFP fluorescence is almost completed during the time elapsed from the end of photobleaching to the beginning of imaging (0.71 seconds). At the same time point the bleaching of ERK2-GFP is still very pronounced, demonstrating a much slower diffusion. Cell stimulation caused a clear decrease in ERK2-GFP mobility, as shown in Fig. 7E by the comparison between the normalized recovery of starved and stimulated cells. We have estimated ERK2-GFP D_{eff} by fitting the recovery with an approximate solution of the diffusion equation (continuous lines) (Feder et al., 1996). The diffusion coefficient of ERK2-GFP is well within the methodology sensitivity and was found to decrease by a factor of two upon stimulation (from 3.1 μm^2/second to 1.6 μm^2/second, Fig. 7F). The small residual recovery of GFP only allowed a rough estimate of a lower limit for GFP diffusion coefficient ($\approx$15 μm^2/second), which is consistent with published values (D_{GFP}>20 μm^2/second) (Chen et al., 2002). The meaning of the IF measured in this experiment is different from the IF found in the whole-nucleus experiment. The IF observed in the whole-nucleus photobleaching measures the fraction of ERK that is unable to leave the nucleus but which is not necessarily immobile within the nucleus. For example, this could be caused by the formation of large complexes to which the membrane is impermeable. By contrast, the spot FRAP experiments measure the fraction that is truly immobilized. These data are consistent because the IF measured in the spot experiments must be $\leqslant$ to the IF measured in the whole-nucleus experiments (starved $IF_{WholeNuc}$=4.0%, IF_{Spot}=3.3%; FGF $IF_{WholeNuc}$=12%, IF_{Spot}=3.2%).

The slow diffusion of ERK2 in the nucleus is probably because of the phosphorylation-dependent binding of ERK2 to sites of low mobility. Since these sites would be saturated by elevated concentrations of ERK2, we should expect that in strongly overexpressing cells most ERK2-GFP would diffuse freely. Since the temporal resolution of the previous assay was insufficient to measure the fluorescence recovery of freely diffusing molecules, we employed a different technique based on the line scan of the cell (Fig. 8A). In this experiment we

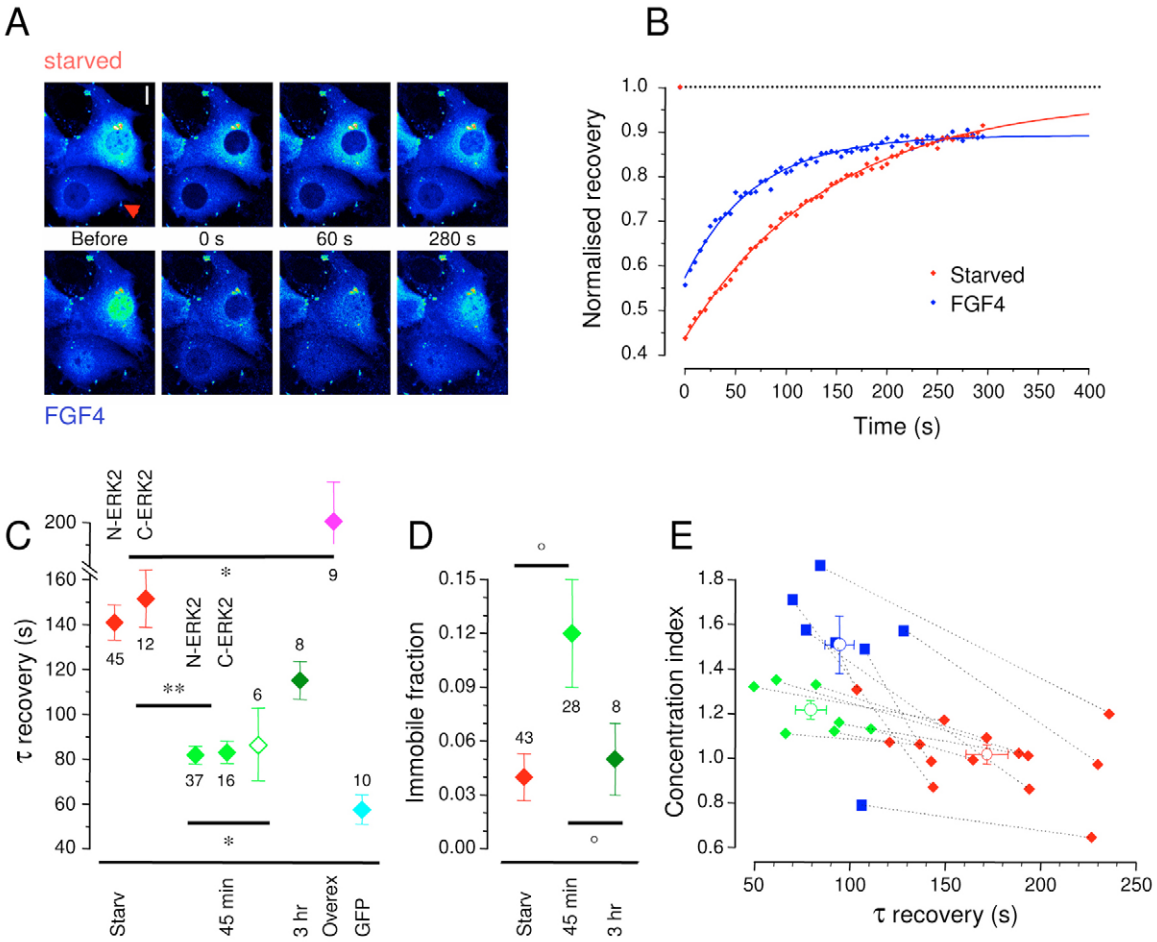

Fig. 6. (A) Fluorescence recovery after photobleaching of the nucleus in starved conditions (upper sequence) and after 30 minutes in FGF4. After the first photobleaching in starved cells, we waited at least 20 minutes to allow complete recovery of fluorescence before proceeding with stimulation and the second photobleaching. Bar, 10 μm. (B) Normalized recovery of the cell indicated by the arrowhead in A. The exponential fit of the fluorescence recovery (continuous lines) is used to compute τ and the IF. Stimulation caused a faster turnover of ERK2-GFP through the nuclear membrane because the τ of the recovery decreased from 144 seconds (red trace) to 69 seconds (blue). A similar effect occurred in the upper cell in A (starved τ=236 seconds; FGF4 τ=84 seconds). (C,D) Averaged τ of recovery and IF for starved cells (red symbols) or after stimulation (45 minutes: green, ERK1-KO: green open; 3 hours: dark green; starved overexpressing: magenta; $^{**}P \leqslant 0.0001$; $^{*}P \leqslant 0.003$; $^{\circ}P \leqslant 0.05$). Time constants have been measured in cells transfected with both the N- and C-terminal fusions. (E) Scatter diagram showing recovery and CI of all paired cells (red, starved; blue, FGF4; green, serum-treated cells). Broken lines join observations relative to the same cell. Open symbols represent averages and s.e.m. of each group.

bleached a thin stripe centred on the nucleus for 300 milliseconds and we imaged the recovery process at high speed. These measures revealed that the fluorescence recovery of ERK2-GFP in strongly overexpressing cells almost overlaps with the recovery of GFP alone (Fig. 8C), confirming that the reduced mobility of ERK2 in the nucleus occurs because of the operation of saturable mechanisms. We have failed to see any phosphorylation-dependent change in mobility in these cells. Since the saturation of MEK1 causes a certain amount of nuclear translocation in overexpressing cells, the low-mobility sites in the nucleus must saturate at a higher concentration of ERK2 than MEK1. In contrast to our data, earlier experiments did not find any difference between the mobility of ERK2-GFP and GFP alone (Burack and Shaw, 2005). Those experiments were performed in strongly overexpressing cells, and therefore the impeded mobility of ERK2 was hidden by the saturation of the binding sites. Once again, this fact highlights the importance of operating on cells minimally perturbed with low levels of expression.

Discussion

We have studied ERK2 localisation and mobility by live imaging of the ERK2-GFP fusion protein. We determined that ERK2-GFP activation and localisation are rapidly and dynamically regulated by concurrent processes of phosphorylation and dephosphorylation that also occur in the absence of substantial extracellular stimulation. This push-pull mechanism exerts a tight control of the protein phosphorylation state that can be regulated bidirectionally within a few minutes by changes in the relative rates of the activation and inactivation processes. Furthermore, since ERK2 is continuously shuttling between the cytoplasm and nucleus at

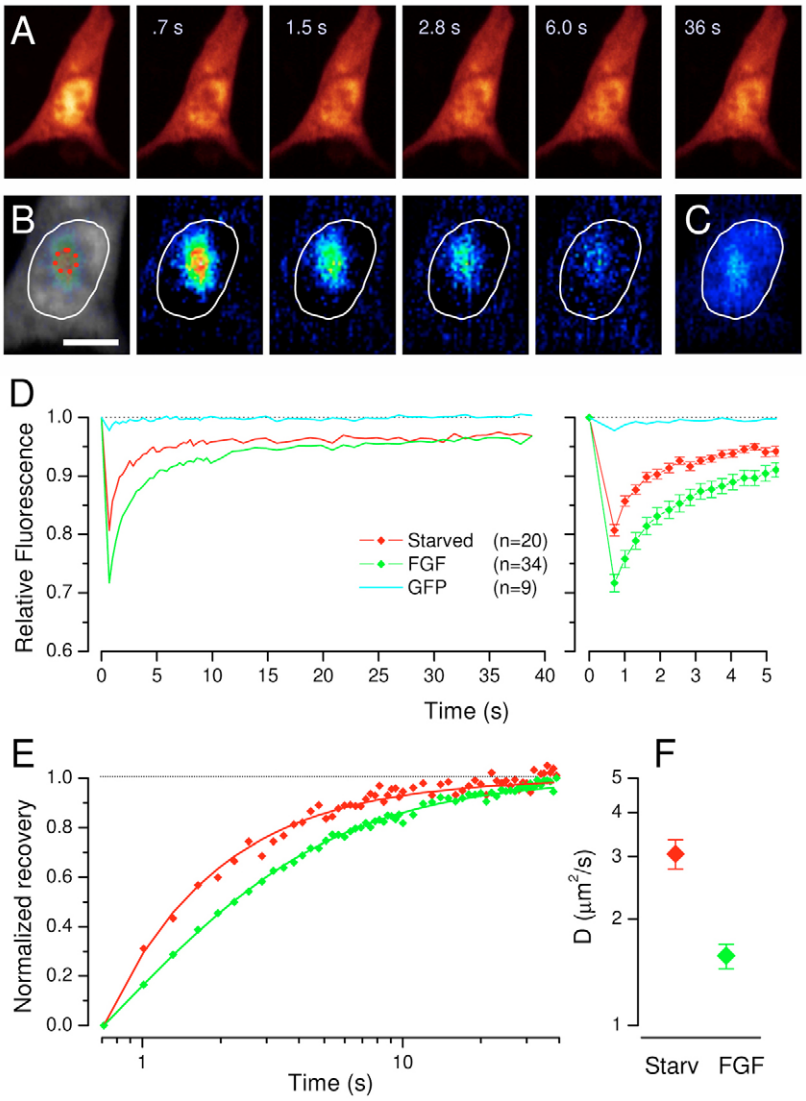

Fig. 7. Reduced mobility of ERK2-GFP in the nucleus. (A) Imaging before photobleaching of a small area of the nucleus (dotted circle in the magnified image in B and at the indicated time during recovery. (B) The false-colour sequence shows the difference with the last frame of the recovery, and therefore the bleached spot disappears as time passes by. Bar, 10 μm. (C) Difference between the pre-bleach image and the last image of the recovery sequence (36 seconds). The signal in the nucleus indicates that the pre-bleach fluorescence is still recovering; this requires slower equilibration through the nuclear envelope. (D) Time course of the normalized fluorescence recovery in the nuclei of starved (red) and stimulated (green) cells. GFP recovery is shown in light blue. Estimate of the asymptotic value reached by the recovery showed the presence of a small but significant IF ($P \leqslant 0.0001$) (percentage of total normalized fluorescence: 3.3±0.6 starved, 3.2±0.7 FGF). (E) ERK activation caused a considerable decrease in the recovery speed. The data in D have been normalized to allow a better comparison of the time course, and have been fitted with an approximate solution of the diffusion equation (solid lines). (F) Computed effective diffusion coefficient for the starved and stimulated cells.

an high rate, the biochemical information coded by its phosphorylation state is rapidly moved between the two compartments. ERK2 is free to leave the nucleus even when the pathway is active and only a small fraction appears to be immobilized in the nucleus, so nuclear accumulation cannot be caused by anchoring to substrates that stably retain ERK2 in the nucleus. However, the transient binding to sites of low mobility is likely to play a role in ERK2 nuclear accumulation since we determined that effective free diffusion of ERK2-GFP in the nucleus is severely limited in an activity-dependent manner.

Nuclear accumulation and shuttling

We have shown that phosphorylation of ERK2-GFP leads to its rapid accumulation in the nucleus and that the duration of the accumulation is related to the temporal pattern of the stimulus and its biochemical identity (Murphy et al., 2004; Murphy et al., 2002; Traverse et al., 1992). Nuclear accumulation is biphasic: a latency phase of approximately 2-4 minutes is followed by rapid accumulation of the protein following an exponential kinetic. The observed lag time correlates well with recent data showing that ERK2 unbinds from MEK1 within 90 seconds of stimulus onset (Burack and Shaw, 2005).

The speed of nuclear accumulation is consistent with the continuous shuttling of ERK2 between the nucleus and cytoplasm. Nuclear accumulation has a substantially slower τ (≈200 seconds) than the shuttling after activation (≈80 seconds) and therefore this process is not a rate-limiting factor. The rate of shuttling, a composite rate of influx, efflux and sequestering in the nucleus, defines the speed of exchange between the two compartments. During nuclear accumulation there is a period in which influx and binding on low-mobility sites prevail over efflux. This imbalance results in the observed change in protein localisation.

Flux of ERK2-GFP across the nuclear envelope cannot occur by simple diffusion through the nuclear pore complex (NPC), since the pore has a diffusion limit of approximately 30-40 kDa (Paine et al., 1975; Bednenko et al., 2003). Therefore, whereas GFP turnover is assured by passive diffusion, other mechanisms must come into play to allow an efficient exchange of ERK2-GFP. The efficiency of these mechanisms

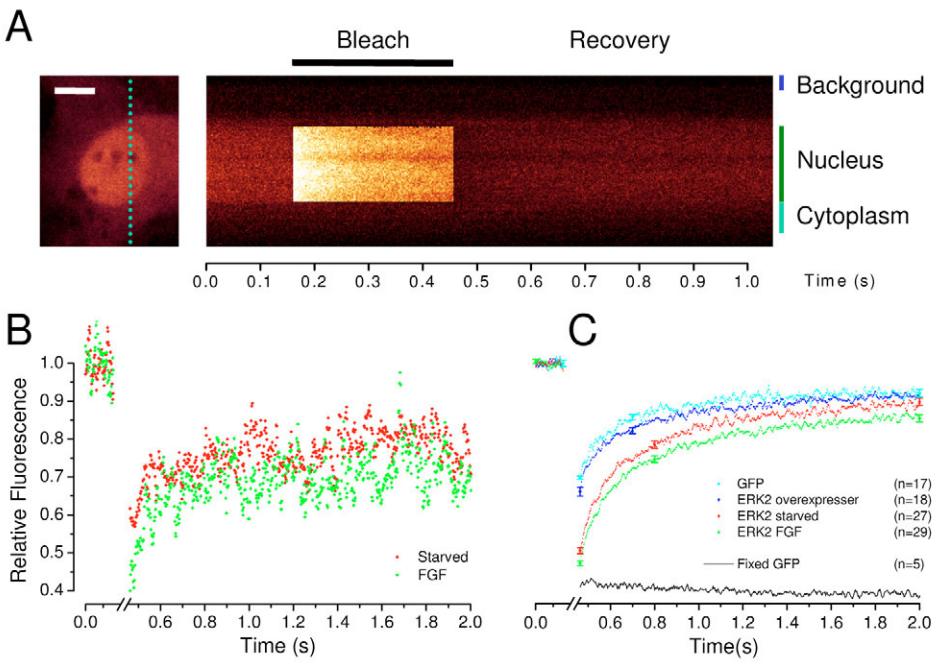

Fig. 8. (A) High-speed FRAP measures. The cell is repeatedly imaged along the broken line at high frequency (400 Hz). Bleaching is performed along a strip covering the nucleus for 300 milliseconds. Fluorescence is corrected for background and divided by the cytoplasm fluorescence to compensate for image bleaching. (B) Recovery of fluorescence for the same cell before (red) and after stimulation with FGF4. Fluorescence has been normalized to the pre-bleach value. (C) Cumulative results. At this temporal resolution the recovery of GFP (starved cells) is clearly discernible and it almost overlaps with the recovery of ERK2-GFP measured in strongly overexpressing cells (blue, stimulation did not cause any change). Photobleaching in low-expressing cells is larger and the recovery is slower, indicating lower mobility, which is dependent on ERK activation.

is witnessed by the fact that the rate of turnover of freely diffusing GFP (58 seconds) is only marginally faster than the turnover of pERK2-GFP, which is much larger (GFP=27 kDa; ERK2-GFP=69 kDa). Two different mechanisms of nuclear entry have been proposed to date (Adachi et al., 1999; Matsubayashi et al., 2001; Whitehurst et al., 2002). First it has been ascertained that ERK2 can diffuse directly though the NPC, since its mass is within the upper limit of diffusion for a globular protein (Adachi et al., 1999). This mode of entry is not available to the larger ERK2-GFP fusion protein (Matsubayashi et al., 2001). A second mode of entry involves the diffusion of ERK2 facilitated by the direct association of the FXF motif of ERK with the NPC (Jacobs et al., 1999). Two different sites of interaction between ERK2 and proteins taking part in the formation of the NPC have been identified: CAN/Nup214 (Matsubayashi et al., 2001) and Nup153 (Whitehurst et al., 2002). Our observation that the rate of shuttling increases after phosphorylation by almost a factor of two can be readily explained by the hypothesis that pERK2 enters by facilitated diffusion of a dimer (Khokhlatchev et al., 1998). Indeed, each dimer would have twice as many binding sites for the nucleoporins and would therefore be twice as likely to cross the channel than ERK2 in monomeric form (Whitehurst et al., 2002). However, a recent report questions the necessity of ERK dimerisation for its translocation (Burack and Shaw, 2005). Indeed, it is possible that the increased shuttling might simply depend on an increased affinity of pERK2 with the consensus sites on the nucleoporins.

Mechanism of ERK2-GFP translocation

Notwithstanding important advances in understanding the mechanisms of ERK2 import and export, the molecular basis of ERK translocation is still somewhat unclear. It is important to remember that ERK overexpression promotes its nuclear localization in starved cells (Fukuda et al., 1997b; Lenormand et al., 1993; Rubinfeld et al., 1999). This piece of evidence is very interesting for two reasons: first, it demonstrates that ERK can accumulate in the nucleus independently of its phosphorylation and kinase activity (Lenormand et al., 1993). Second, the relative reduction in MEK-CRM1 export that occurs because of overexpression of ERK or after treatment with leptomycin B (Adachi et al., 1999) (see also supplementary material Fig. S7) does not end with a zero gradient across the nuclear envelope but progresses to accumulation. This evidence suggests that ERK2 would accumulate inside the nucleus regardless of its phosphorylation state and that the cytosolic retention observed in starved cells is maintained by the CRM1-mediated export (Adachi et al., 2000; Fukuda et al., 1997b). The tendency of ERK to accumulate in the nucleus can be explained by two different mechanisms that are not mutually exclusive: (1) the import can proceed against a concentration gradient; (2) imported ERK binds to nuclear anchoring proteins that do not allow its export and/or impede its free diffusion.

Facilitated diffusion of ERK across the nuclear envelope (Matsubayashi et al., 2001; Whitehurst et al., 2002) does not require energy and therefore it cannot create a gradient of free concentration across the nuclear envelope (Bednenko et al., 2003). Although it has been reported that dimeric pERK can be actively imported by a Ran-dependent active transport (Adachi et al., 1999), the import and nuclear accumulation of ERK2-GFP is energy independent and does not occur through this mechanism (Matsubayashi et al., 2001; Whitehurst et al., 2002; Burack and Shaw, 2005). Therefore, the available data require the presence of some nuclear anchoring proteins operating on ERK. The molecular identity of these molecules is still to be identified and it is possible that several partners are involved. Part of the anchoring system might be formed by short-lived nuclear anchoring proteins expressed in response to ERK activation (Lenormand et al., 1998). The anchoring system probably also includes products of immediate early genes (such as *Fos*, *Jun*, *Myc*) that have functional docking

sites for ERK (Murphy et al., 2004). Although translation-based mechanisms are crucial for the long-term nuclear sequestration of ERK (>3 hours), they are not likely to play a substantial role within the timescale of the processes we studied (≤1 hour) and certainly not during the rapid onset of translocation. It is likely that this process also involves high-affinity interactions with low-mobility sites that are constitutively expressed. We have shown that in starved cells nuclear accumulation progresses with increasing concentration of ERK-GFP, until reaching a plateau at approximately 1.5 μM. Since the endogenous concentration of ERK is approximately 1-3 μM (Ferrell, Jr, 1996; Whitehurst et al., 2002), our data suggest that the concentration of the nuclear anchoring system is in the range of 2-5 μM.

The combination of the shuttling and fast FRAP experiments demonstrates that the anchoring should not be seen as a stable retention of ERK inside the nucleus, since only a modest percentage of total ERK2-GFP (12%) is immobilized in the nucleus after activation. This fraction is far too small to explain the observed translocation. Furthermore, we have shown that the fraction of immobilized ERK-GFP in an overexpressing cell, where there is conspicuous nuclear accumulation, is negligible. Most of the nuclear anchoring is therefore rapidly reversible: in these conditions a fraction of ERK2 is transiently bound to substrates of low mobility and the free concentration of ERK2 in the nucleus is less than its total concentration. The diffusion coefficient of freely diffusing solutes depends only weakly on the molecular mass since it is proportional to 1/cubic root (mass) as predicted by the Stokes-Einstein equation (Seksek et al., 1997). If ERK2-GFP were freely diffusing we would expect the following sequence of relative diffusion coefficients: GFP (27 kD): 1; ERK2 (42 kD): 0.86; ERK2-GFP (69 kD): 0.73; MEK-ERK2-GFP (116 kD): 0.62; dimer ERK2-GFP (138 kD): 0.58. There are various estimates of GFP diffusion coefficient in the nucleus, with values ranging from 23 to 58 μm^2/second (Chen et al., 2002; Houtsmuller et al., 1999; Yokoe and Meyer, 1996). Taking the smallest value of these estimates, if ERK2-GFP were freely diffusible we would expect a diffusion coefficient in the range of 14-17 μm^2/second. Our estimate (≈3 μm^2/second) suggests that diffusion of ERK2-GFP in the nucleus of starved cells is far more restricted than simple Brownian diffusion. This dichotomy is further reinforced after stimulation when the predicted D_{eff} of the ERK2-GFP dimer (13 μm^2/second) is almost ten times larger than our estimate (1.5 μm^2/second). These data demonstrate that, although ERK2-GFP is mobile and can leave the nucleus, free diffusion is impeded within the nucleus and that this limitation in mobility is increased after stimulation. The reduced mobility of ERK2-GFP helps to explain the tendency of ERK to accumulate inside the nucleus in the absence of an efficient means of active export.

Dynamical regulation of ERK phosphorylation

The emerging picture is one of a highly dynamic system in which ERK2 continuously shuttles between the cytoplasm and the nucleus. This rapid exchange between the cytosolic and nuclear compartments is associated with a continuous dephosphorylation of ERK in the nucleus (Volmat et al., 2001). The nuclear concentration of ERK is determined by the balance between activity-dependent influx and efflux and binding to low-mobility sites. Blockage of MEK1 by U0126 showed that ERK2-GFP abandons the nucleus with a τ of 3 minutes, suggesting that two-thirds of nuclear pERK is dephosphorylated every 3 minutes. Therefore, even during the sustained translocation caused by FGF4 a fraction of nuclear ERK is dephosphorylated. Indeed, orthovanadate caused an increase in the CI even in the presence of a saturating amount of FGF4. The rapidity of the phosphorylation and dephosphorylation turnover together with the rapid shuttling of ERK allows for rapid changes of ERK phosphorylation, and this biochemical information is promptly transferred between the nucleo-cytoplasmic compartments (Xu and Massague, 2004). Our data reveal a fast dynamic aspect of ERK regulation and localization that was hitherto ignored.

ERK inactivation is dependent on several different phosphatases of varying selectivity and cellular localization. In particular, dual-specificity phosphatases MKP1 and MKP2 are localized in the nucleus (Brondello et al., 1995), their level of expression is regulated by ERK activity (Brondello et al., 1997; Brondello et al., 1999) and they are endowed with docking sites for ERK (Camps et al., 2000). Indeed, it has been proposed that they participate in the ERK nuclear anchoring system (reviewed by Pouyssegur et al., 2002). Since we observed that ERK dephosphorylation is rapidly recruited after stimulation (within 15 minutes), the capability of MKP1/2 to participate in ERK inactivation so early after stimulation depends crucially on their basal level of expression and on the rapidity of their transcription and activation. Indeed, computational studies reveal that such mutual interactions limit and regulate levels and the time course of ERK activation (Bhalla and Iyengar, 1999; Bhalla et al., 2002). It is likely that the low-mobility binding sites for ERK are provided by interactions with downstream kinases, anchoring proteins and phosphatases, creating a highly dynamic system controlling mobility and activation of the ERK pathway. Given the fast regulation of ERK nuclear mobility it seems likely that some of these regulatory processes must occur through non-transcriptional systems.

We have shown that ERK produces a steady response to a constant stimulus through highly dynamic regulation. This system is potentially capable of controlling gene expression or other targets with noteworthy rapidity and temporal fidelity to the activation kinetic of the upstream pathway. Interestingly, it has recently been shown that the transcriptional effects of activated ERK on MKP expression can already be detected 15-30 minutes after stimulation (Bhalla et al., 2002). This regulatory mechanism implies that, in the appropriate context, the degree of ERK activation and its translocation might follow complex temporal patterns with a bandwidth of few minutes and that ERK might undergo burst-like episodes of activation lasting 15-20 minutes. The existence of such rapidly modulated activity has still to be observed but this might simply reflect the limits of the techniques employed so far. Novel experimental paradigms will have to be developed to uncover these processes and their relevance for cell physiology.

Materials and Methods

Plasmid preparation

One-step reverse transcription-polymerase chain reaction (RT-PCR) was performed with a template on 100 ng of total RNA extract from mice brain. The forward primer was 5′-ACGTCTCGAGATGCTGTGCAGCCAAC**ATG**G-3′, incorporating *Xho*I site (underlined) and the ERK2 ATG start codon (bold). The reverse primer was 5′-ACGTGGATCC**TTA**AGATCTGTATCCTGGC-3′ incorporating *Bam*HI site (underlined) and the ERK2 stop codon (bold). The amplification product was

purified and cleaved with *Xho*I/*Bam*HI, and ligated to the corresponding restriction site in the Clontech vectors pEGFP-C2 or pYFP-C1 to fuse the fluorescent reporter to the N-terminus of ERK2 (N-ERK). The C-terminal fusion protein was obtained by PCR amplification removing the ERK stop codon from the reverse primer. The amplification product was ligated to the pYFP-N1 vector (C-ERK). Verification of correct sequence and framing was obtained from forward and reverse automated fluorescence sequencing. Most experiments were performed with the N-terminal fusion with either GFP or yellow fluorescent protein (YFP) with identical results. Selected experiments were performed with the C-ERK fusion with identical results.

Cell culture and transfection

The NIH-3T3 cell line was cultured in modified Dulbecco's medium supplemented with 10% fetal bovine serum (FBS) and antibiotics (100 units/ml penicillin-streptomycin). The cells were plated on glass disks that were 14 mm in diameter at 60-70% confluence, and transfected using Lipofectamine (GenePORTER 2; Genlantis, San Diego, CA). After transfection, cells were left undisturbed for 24 hours before any further experimental manipulation. Cells were starved by keeping them in 1% FBS for 24 hours. One hour prior to the start of the experiment, cells were placed in a saline solution of: 130 mM NaCl, 3.1 mM KCl, 1.0 mM K_2HPO_4, 4.0 mM $NaHCO_3$, 5.0 mM dextrose, 1.0 mM $MgCl_2$, 2.0 mM $CaCl_2$, 10 mM HEPES, 1.0 mM ascorbic acid, 0.5 mM myo-inositol, 2 mM pyruvic acid, pH 7.3. All experiments were performed at 25°C.

Immunocytochemistry and immunoblotting

Cells were fixed in Tris buffer containing 4% formaldehyde, 1 mM vanadate and 30% glucose at room temperature for 10 minutes, and then washed three times with blocking solution [0.4% Triton X-100, 10% bovine serum albumin (BSA), 10 mM Tris and 1 mM sodium orthovanadate]. Coverslips were incubated overnight with a phosphospecific ERK1/2 antibody (dilution 1:1000, Sigma M-8159) in blocking solution at 4°C. The reaction was completed by incubation for 2 hours in secondary antibody (Alexa Fluor 546, Molecular Probes).

Imaging

Immunohistochemistry acquisition, time-lapse imaging and nuclear FRAP experiments were all performed with an Olympus Fluoview 300 confocal scanning head, mounted on an upright microscope with a water immersion lens (Olympus WLSM 60×, N.A. 0.9). The unit was equipped with visible light and with an infrared laser for 2-photon excitation (Verdi-Mira; Coherent). Fast-FRAP experiments were performed on a Leica TCS NT (spot FRAP) or a Leica SL (strip FRAP) confocal microscope equipped with a water immersion lens (Leica HCX PL APO 63×, N.A. 0.9). In all experiments GFP fluorescence was excited at 488 nm. Acquisition of pERK immunohistochemistry was performed on randomly chosen fields by blind operators. Combined imaging of pERK immunofluorescence and ERK2-GFP fluorescence was performed separately for the two channels to minimize cross talk. Quantification of fluorescence was performed either on the Fluoview platform or with custom software.

Coverslips were placed in a recording chamber filled with a 0.7 ml volume of saline solution. Cells were carefully selected by measuring the fluorescence of ERK2-GFP; cells characterized by medium-high levels of expression were avoided (Fig. 1). Given the weak fluorescence and the need to contain photobleaching, we optimized detection sensitivity by fully opening the confocal aperture and using a wide-emission bandpass. These conditions caused the frequent presence of fluorescent debris overimposed on the cells. During quantification of fluorescence these points were avoided. Average fluorescence background was evaluated on non-transfected cells and was subtracted from all measurements.

To evaluate the degree of nuclear localization we measured the average fluorescence of the nucleus (F_{Nuc}) and of a surrounding ring of thickness approximately equal to the nucleus radius (F_{Ring}). The CI was computed as:

$$CI = (F_{Nuc}–BG)/(F_{Ring}–BG)\ , \tag{1}$$

where *BG* was the average background. All images shown in the study have been subjected only to linear adjustments. Data plotting and statistical testing (one- or two-way *t*-test) was been performed with Origin 7. Other statistical tests were used where appropriate. Quality of fits was given by the correlation coefficient R^2.

FRAP experiments: nucleus-cytoplasm shuttling

Photobleaching was preceded by the acquisition of a pre-bleach image that was used to estimate the loss of fluorescence due to bleaching and for data normalization. The nucleus of the cell was photobleached by repeated scans along a line centred on the nucleus at high laser power. Bleaching was applied for approximately 8 seconds, which was sufficient to quench most of the nuclear fluorescence. This indicates that the typical time for the mixing of ERK2-GFP in the nucleus is <10 seconds. Bleaching was followed by time-lapse acquisition to measure the recovery (60 frames at 5-second intervals). Recovery was described by the function

$$F(t) = \frac{F^{PB}_{Tot}}{F^{PB}_{Nuc}} \times \frac{F_{Nuc}(t)}{F_{Tot}(t)}\ , \tag{2}$$

where F^{PB} indicates the fluorescence (corrected for background) measured before bleaching in the nucleus (*Nuc*) or on the entire cell (*Tot*). This normalization corrects for bleaching caused by imaging (Phair and Misteli, 2000). In the absence of IF, the formula has an asymptotic value of one. The recovery of all imaged cells was accurately fitted with a single exponential defined by the time constant τ of shuttling and by the IF (asymptotic value).

FRAP experiments: spot photobleaching

Spot photobleaching was attained by flashing a diffraction-limited spot in a fixed position near to the nucleus center for 250 milliseconds. Recovery was measured in a time-lapse sequence imaged immediately afterwards. Owing to the technical limitations of the scanning-head, the shortest interval elapsing from the end of bleaching until the beginning of recovery was 0.71 seconds, as determined by direct measurements with a photodiode. This delay prevented a meaningful measurement of the recovery of freely diffusible GFP in the nuclear compartment. The spatial profile of the bleached area was measured on fixed cells bleached in the same conditions as in the in vivo experiments. Normalized fluorescence was fitted by the equation provided by Axelrod et al. (Axelrod et al., 1976):

$$F(x) = e^{-Ke^{-\left(\frac{x}{w}\right)^2}}\ , \tag{3}$$

where *K* defines the depth of the photobleaching and *w* its width. The mean values for these parameters were found to be K=1.63±0.10, w=2.02±0.18 μm (n=8).

The effective diffusion coefficient D_{eff} was computed by fitting the recovery data to an approximate solution of the diffusion equation (Feder et al., 1996):

$$I(t) = \frac{I_0 + I_\infty \frac{t}{t_{1/2}}}{1+\frac{t}{t_{1/2}}}\ , \tag{4}$$

where I_0 and I_∞ are the fluorescence intensity at time zero and at the asymptote. The time to half recovery $t_{1/2}$ depends on the diffusion coefficient D_{eff}, and on the width *w* of the bleaching through the relationship:

$$t_{1/2} = \frac{w^2\gamma}{2D_{eff}}\ , \tag{5}$$

where the factor γ is a weak function of the beam shape and of the bleach depth *K*; in our experiments γ=1.1 (Axelrod et al., 1976; Carrero et al., 2003).

The study was funded by CaRiPi (139/03) and by the International Foundation for Paraplegia (IFP P82). We are grateful to Riccardo Brambilla and Ivan Formentini for the ERK1-KO cell line, to Margherita Maffei, Claudio Basilico and Yuri Bozzi for providing reagents and to Riccardo Parra and Sebastian Sulis-Sato for participation in data analysis. A.R. was supported by ASICTP (Trieste, Italy) through an ICTP TRIL fellowship.

References

Adachi, M., Fukuda, M. and Nishida, E. (1999). Two co-existing mechanisms for nuclear import of MAP kinase: passive diffusion of a monomer and active transport of a dimer. *EMBO J.* **18**, 5347-5358.

Adachi, M., Fukuda, M. and Nishida, E. (2000). Nuclear export of MAP kinase (ERK) involves a MAP kinase kinase (MEK)-dependent active transport mechanism. *J. Cell Biol.* **148**, 849-856.

Ando, R., Mizuno, H. and Miyawaki, A. (2004). Regulated fast nucleocytoplasmic shuttling observed by reversible protein highlighting. *Science* **306**, 1370-1373.

Axelrod, D., Koppel, D. E., Schlessinger, J., Elson, E. and Webb, W. W. (1976). Mobility measurement by analysis of fluorescence photobleaching recovery kinetics. *Biophys. J.* **16**, 1055-1069.

Bednenko, J., Cingolani, G. and Gerace, L. (2003). Nucleocytoplasmic transport: navigating the channel. *Traffic* **4**, 127-135.

Bhalla, U. S. and Iyengar, R. (1999). Emergent properties of networks of biological signaling pathways. *Science* **283**, 381-387.

Bhalla, U. S., Ram, P. T. and Iyengar, R. (2002). MAP kinase phosphatase as a locus of flexibility in a mitogen-activated protein kinase signaling network. *Science* **297**, 1018-1023.

Brondello, J. M., McKenzie, F. R., Sun, H., Tonks, N. K. and Pouyssegur, J. (1995). Constitutive MAP kinase phosphatase (MKP-1) expression blocks G1 specific gene transcription and S-phase entry in fibroblasts. *Oncogene* **10**, 1895-1904.

Brondello, J. M., Brunet, A., Pouyssegur, J. and McKenzie, F. R. (1997). The dual specificity mitogen-activated protein kinase phosphatase-1 and -2 are induced by the p42/p44MAPK cascade. *J. Biol. Chem.* **272**, 1368-1376.

Brondello, J. M., Pouyssegur, J. and McKenzie, F. R. (1999). Reduced MAP kinase phosphatase-1 degradation after p42/p44MAPK-dependent phosphorylation. *Science* **286**, 2514-2517.

Brunet, A., Roux, D., Lenormand, P., Dowd, S., Keyse, S. and Pouyssegur, J. (1999). Nuclear translocation of p42/p44 mitogen-activated protein kinase is required for growth factor-induced gene expression and cell cycle entry. *EMBO J.* **18**, 664-674.

Burack, W. R. and Shaw, A. S. (2005). Live cell imaging of ERK and MEK: simple binding equilibrium explains the regulated nucleocytoplasmic distribution of ERK. *J. Biol. Chem.* **280**, 3832-3837.
Camps, M., Nichols, A. and Arkinstall, S. (2000). Dual specificity phosphatases: a gene family for control of MAP kinase function. *FASEB J.* **14**, 6-16.
Carrero, G., McDonald, D., Crawford, E., de Vries, G. and Hendzel, M. J. (2003). Using FRAP and mathematical modeling to determine the in vivo kinetics of nuclear proteins. *Methods* **29**, 14-28.
Chen, R. H., Sarnecki, C. and Blenis, J. (1992). Nuclear localization and regulation of erk- and rsk-encoded protein kinases. *Mol. Cell. Biol.* **12**, 915-927.
Chen, Y., Muller, J. D., Ruan, Q. and Gratton, E. (2002). Molecular brightness characterization of EGFP in vivo by fluorescence fluctuation spectroscopy. *Biophys. J.* **82**, 133-144.
Chuderland, D. and Seger, R. (2005). Protein-protein interactions in the regulation of the extracellular signal-regulated kinase. *Mol. Biotechnol.* **29**, 57-74.
Cowley, S., Paterson, H., Kemp, P. and Marshall, C. J. (1994). Activation of MAP kinase kinase is necessary and sufficient for PC12 differentiation and for transformation of NIH 3T3 cells. *Cell* **77**, 841-852.
English, J. M. and Cobb, M. H. (2002). Pharmacological inhibitors of MAPK pathways. *Trends Pharmacol. Sci.* **23**, 40-45.
Feder, T. J., Brust-Mascher, I., Slattery, J. P., Baird, B. and Webb, W. W. (1996). Constrained diffusion or immobile fraction on cell surfaces: a new interpretation. *Biophys. J.* **70**, 2767-2773.
Ferrell, J. E., Jr (1996). Tripping the switch fantastic: how a protein kinase cascade can convert graded inputs into switch-like outputs. *Trends Biochem. Sci.* **21**, 460-466.
Fukuda, M., Gotoh, I., Adachi, M., Gotoh, Y. and Nishida, E. (1997a). A novel regulatory mechanism in the mitogen-activated protein (MAP) kinase cascade. Role of nuclear export signal of MAP kinase kinase. *J. Biol. Chem.* **272**, 32642-32648.
Fukuda, M., Gotoh, Y. and Nishida, E. (1997b). Interaction of MAP kinase with MAP kinase kinase: its possible role in the control of nucleocytoplasmic transport of MAP kinase. *EMBO J.* **16**, 1901-1908.
Horgan, A. M. and Stork, P. J. (2003). Examining the mechanism of Erk nuclear translocation using green fluorescent protein. *Exp. Cell Res.* **285**, 208-220.
Houtsmuller, A. B., Rademakers, S., Nigg, A. L., Hoogstraten, D., Hoeijmakers, J. H. and Vermeulen, W. (1999). Action of DNA repair endonuclease ERCC1/XPF in living cells. *Science* **284**, 958-961.
Jacobs, D., Glossip, D., Xing, H., Muslin, A. J. and Kornfeld, K. (1999). Multiple docking sites on substrate proteins form a modular system that mediates recognition by ERK MAP kinase. *Genes Dev.* **13**, 163-175.
Khokhlatchev, A. V., Canagarajah, B., Wilsbacher, J., Robinson, M., Atkinson, M., Goldsmith, E. and Cobb, M. H. (1998). Phosphorylation of the MAP kinase ERK2 promotes its homodimerization and nuclear translocation. *Cell* **93**, 605-615.
Kim, K., Nose, K. and Shibanuma, M. (2000). Significance of nuclear relocalization of ERK1/2 in reactivation of c-fos transcription and DNA synthesis in senescent fibroblasts. *J. Biol. Chem.* **275**, 20685-20692.
Koster, M., Frahm, T. and Hauser, H. (2005). Nucleocytoplasmic shuttling revealed by FRAP and FLIP technologies. *Curr. Opin. Biotechnol.* **16**, 28-34.
Kudo, N., Taoka, H., Toda, T., Yoshida, M. and Horinouchi, S. (1999). A novel nuclear export signal sensitive to oxidative stress in the fission yeast transcription factor Pap1. *J. Biol. Chem.* **274**, 15151-15158.
Lenormand, P., Sardet, C., Pages, G., L'Allemain, G., Brunet, A. and Pouyssegur, J. (1993). Growth factors induce nuclear translocation of MAP kinases (p42mapk and p44mapk) but not of their activator MAP kinase kinase (p45mapkk) in fibroblasts. *J. Cell Biol.* **122**, 1079-1088.
Lenormand, P., Brondello, J. M., Brunet, A. and Pouyssegur, J. (1998). Growth factor-induced p42/p44 MAPK nuclear translocation and retention requires both MAPK activation and neosynthesis of nuclear anchoring proteins. *J. Cell Biol.* **142**, 625-633.
Lippincott-Schwartz, J., Snapp, E. and Kenworthy, A. (2001). Studying protein dynamics in living cells. *Nat. Rev. Mol. Cell Biol.* **2**, 444-456.
Matsubayashi, Y., Fukuda, M. and Nishida, E. (2001). Evidence for existence of a nuclear pore complex-mediated, cytosol-independent pathway of nuclear translocation of ERK MAP kinase in permeabilized cells. *J. Biol. Chem.* **276**, 41755-41760.
Murphy, L. O., Smith, S., Chen, R. H., Fingar, D. C. and Blenis, J. (2002). Molecular interpretation of ERK signal duration by immediate early gene products. *Nat. Cell Biol.* **4**, 556-564.
Murphy, L. O., MacKeigan, J. P. and Blenis, J. (2004). A network of immediate early gene products propagates subtle differences in mitogen-activated protein kinase signal amplitude and duration. *Mol. Cell. Biol.* **24**, 144-153.
Paine, P. L., Moore, L. C. and Horowitz, S. B. (1975). Nuclear envelope permeability. *Nature* **254**, 109-114.
Phair, R. D. and Misteli, T. (2000). High mobility of proteins in the mammalian cell nucleus. *Nature* **404**, 604-609.
Pouyssegur, J., Volmat, V. and Lenormand, P. (2002). Fidelity and spatio-temporal control in MAP kinase (ERKs) signalling. *Biochem. Pharmacol.* **64**, 755-763.
Robinson, M. J. and Cobb, M. H. (1997). Mitogen-activated protein kinase pathways. *Curr. Opin. Cell Biol.* **9**, 180-186.
Robinson, M. J., Stippec, S. A., Goldsmith, E., White, M. A. and Cobb, M. H. (1998). A constitutively active and nuclear form of the MAP kinase ERK2 is sufficient for neurite outgrowth and cell transformation. *Curr. Biol.* **8**, 1141-1150.
Roux, P. P. and Blenis, J. (2004). ERK and p38 MAPK-activated protein kinases: a family of protein kinases with diverse biological functions. *Microbiol. Mol. Biol. Rev.* **68**, 320-344.
Rubinfeld, H., Hanoch, T. and Seger, R. (1999). Identification of a cytoplasmic-retention sequence in ERK2. *J. Biol. Chem.* **274**, 30349-30352.
Schramek, H., Schumacher, M. and Pfaller, W. (1996). Sustained ERK-2 activation in rat glomerular mesangial cells: differential regulation by protein phosphatases. *Am. J. Physiol.* **271**, F423-F432.
Seksek, O., Biwersi, J. and Verkman, A. S. (1997). Translational diffusion of macromolecule-sized solutes in cytoplasm and nucleus. *J. Cell Biol.* **138**, 131-142.
Traverse, S., Gomez, N., Paterson, H., Marshall, C. and Cohen, P. (1992). Sustained activation of the mitogen-activated protein (MAP) kinase cascade may be required for differentiation of PC12 cells. Comparison of the effects of nerve growth factor and epidermal growth factor. *Biochem. J.* **288**, 351-355.
Vantaggiato, C., Formentini, I., Bondanza, A., Bonini, C., Naldini, L. and Brambilla, R. (2006). ERK1 and ERK2 mitogen-activated protein kinases affect Ras-dependent cell signaling differentially. *J. Biol.* **5**, 14.
Volmat, V., Camps, M., Arkinstall, S., Pouyssegur, J. and Lenormand, P. (2001). The nucleus, a site for signal termination by sequestration and inactivation of p42/p44 MAP kinases. *J. Cell Sci.* **114**, 3433-3443.
Whitehurst, A. W., Wilsbacher, J. L., You, Y., Luby-Phelps, K., Moore, M. S. and Cobb, M. H. (2002). ERK2 enters the nucleus by a carrier-independent mechanism. *Proc. Natl. Acad. Sci. USA* **99**, 7496-7501.
Xu, L. and Massague, J. (2004). Nucleocytoplasmic shuttling of signal transducers. *Nat. Rev. Mol. Cell Biol.* **5**, 209-219.
Yokoe, H. and Meyer, T. (1996). Spatial dynamics of GFP-tagged proteins investigated by local fluorescence enhancement. *Nat. Biotechnol.* **14**, 1252-1256.